

ARTICLE

Tuning the surface energies in a family of poly-3-alkylthiophenes bearing hydrophilic side-chains synthesized via direct arylation polymerization (DArP)

Received 00th January 20xx,
Accepted 00th January 20xx

DOI: 10.1039/x0xx00000x

Alexander Schmitt, Sanket Samal, Barry C. Thompson*^a

Recent work has identified surface energy as a key figure of merit in predicting the morphology of bulk heterojunction organic solar cells and organic alloy formation in ternary blend organic solar cells. An efficient way of tuning surface energy in conjugated polymers is by introducing functionalised side chains. Here, we present a systematic study on a family of poly(3-hexylthiophene) (P3HT)-based random copolymers bearing five different functionalised side chains (ester, ether, diether, carbamate, nitrile) prepared by direct arylation polymerization (DArP) in terms of their effectiveness in tuning surface energy. This study also exemplifies the superior functional group tolerance in DArP compared to more traditional polymerization procedures. Water droplet contact angle measurements revealed that especially carbamates are highly effective in tuning surface energy, increasing the surface energy from 21.2 mN/m with P3HT to 25.5 mN/m and 28.6 mN/m in 25% and 50% carbamate functionalized copolymers, respectively. Importantly, by introducing a two-carbon-spacer between the conjugated backbone and the functional group, optical and electronic properties of P3HT could be largely maintained in the copolymers as determined by UV/Vis, cyclic voltammetry and space charge limited current hole mobility.

Introduction

Conjugated polymers are a promising class of materials that enable the fabrication of cost efficient, flexible, and solution-processable devices such as organic photovoltaics (OPVs), stretchable organic electronics and sensors, as well as organic field effect transistors (OFETs).¹⁻⁸ Specifically, they are a vital component in bulk heterojunction (BHJ) organic solar cells which commonly feature a polymer donor coupled with an acceptor material such as a fullerene or non-fullerene-derived small molecule or a polymer.^{1,9,10}

Recently reported examples of such traditional binary BHJ solar cells are approaching the practical efficiency limitations of the platform.¹¹⁻¹⁴ One of the most extensively studied strategies proposed to increase the achievable efficiency in both polymeric and small molecule systems is the ternary blend solar cell which contains either one donor with two acceptors (D/A₁/A₂) or two donors with a single acceptor (D₁/D₂/A).¹⁵⁻¹⁷ These systems benefit from the same simple and straight forward fabrication and processing already established for binary blend-BHJ solar cells. Importantly, the addition of a third photoactive component can lead to an estimated 40% increase in efficiency.¹⁸ This enhancement is enabled by broadening of the absorption spectra and the resulting improved short-circuit photocurrents (J_{SC}) as well as a compositionally tuneable open-

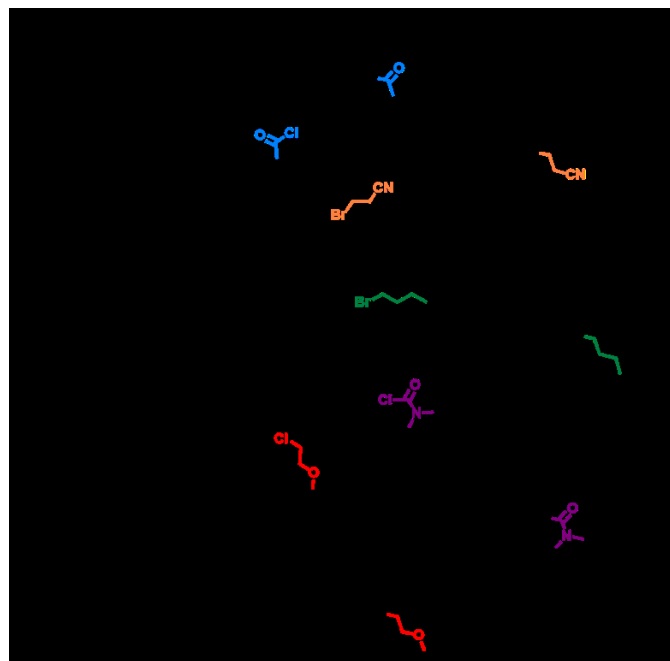
circuit voltage (V_{OC}) based on the ratio of the two donors/acceptors mixed in the active layer.¹⁹⁻²⁴

However, not all ternary blends lead to both an enhancement in J_{SC} and a composition-dependent V_{OC}. In many cases, the ternary cell exhibits a V_{OC} that is pinned to the lower V_{OC} of the limiting binary constituents. In these cases, the cell voltage is limited by the higher of the two highest occupied molecular orbitals (HOMOs) of the donors (in the D₁/D₂/A case) or the lower of the two lowest unoccupied molecular orbitals (LUMOs) of the acceptors (in the D/A₁/A₂ case) and thus the smallest possible HOMO-LUMO offset in the given active layer.^{25,26} Because the third component typically features a narrower bandgap, the resulting V_{OC} in these pinned systems is limited to the lower of the two constituent binary blends, thus minimizing the impact of the ternary approach.^{27,28} The majority of previous work supports that a tuneable voltage in ternary blends can only be realised through a controlled active layer morphology allowing for intimate mixing of the synergistic components, either the two donors or the two acceptors, in this layer.²⁹⁻³⁷ Only such intimate mixing of the synergistic components facilitates the formation of a new phase in the active layer, termed an organic alloy by Thompson *et al.*, which will then allow for a tuneable voltage for the respective blend.^{21,22,29,38,39} In previous studies, surface energy, γ , has been identified as a key figure of merit for predicting the degree of mixing of synergistic components in the active layer. As reported by Thompson *et al.*²⁹⁻³¹, Yan *et al.*³² and Zhu *et al.*³³ closely matched surface energies of the synergistic components is required to achieve the intimate mixing necessary to control the active layer morphology.

^a Department of Chemistry and Loker Hydrocarbon Research Institute, University of Southern California, Los Angeles, California 90089-1661, USA.

^b Footnotes relating to the title and/or authors should appear here.

Electronic Supplementary Information (ESI) available: [details of any supplementary information available should be included here]. See DOI: 10.1039/x0xx00000x



Scheme 1: Synthesis of comonomers 2-6.

In a more general sense, beyond ternary blends, the surface energy of components has been demonstrated as a strong predictor of morphology in BHJ solar cells by *Brabec et al.*^{40,41}, *Zhou et al.*⁴² and *Lee et al.*⁴³ amongst others and thus exploring methods of tuning surface energies in polymeric and molecular components is an important avenue of research.^{44,45}

As such, it is critical to develop effective synthetic approaches for polymeric and molecular components with precisely tailored surface energies. In our past work we have shown that modification of polymer side chains is an effective method of tuning the surface energy, where we used random poly(3-alkylthiophene) copolymers as model systems.^{30,31} Specifically, we found that introduction of hydrophilic oligoether side chains allowed for an increase in surface energy of about 7 mN/m and hydrophobic polyfluorinated side chains allowed for a decrease of about 5 mN/m relative to P3HT.^{30,31} *Jen et al.* also successfully employed terminal nitriles to increase surface energy in their thiophene-flanked diketopyrrolopyrrole system⁴⁶ while *Chen et al.* saw an increase in surface energy for PTB7-Th-based polymers when siloxane capped side chains were introduced⁴⁷

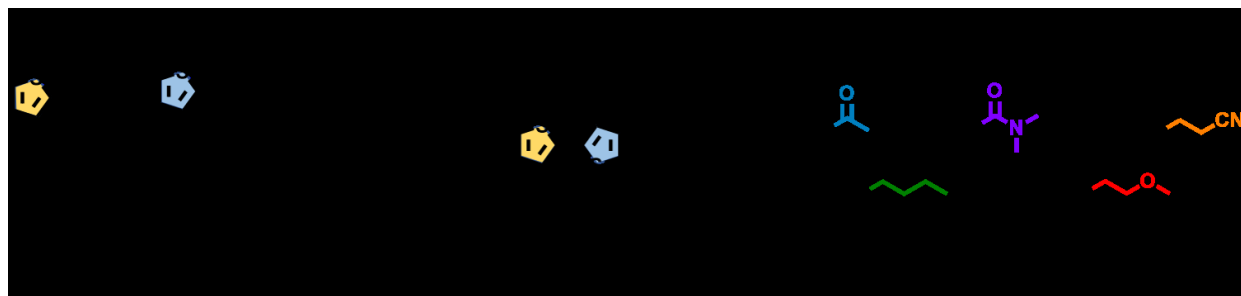
and *Heeney et al.* were able to gradually increase the wettability of (poly(diethylfluorene-co-benzothiadiazole)) through incorporation of ethylene glycol oligomers of varying length.⁴⁸

While these examples clearly demonstrate that side chain engineering is a suitable tool for tuning surface energies in polymers, to the best of our knowledge there are no studies to date on broader families of functionalised side chains to compare the degree of surface energy tuning facilitated by these functional groups. Consequently, the choice of functionalised side chain for surface energy tuning is largely random, based on a trial-and-error approach.

Herein, we report a model family of random poly(3-alkylthiophene) copolymers featuring five different functionalised side chains synthesized by direct arylation polymerization (DAP). Each functionalised side chain is incorporated in random poly(3-hexithiophene) (P3HT)-copolymers in 25% and 50% ratios. This allows us to compare the degree of surface energy tuning facilitated by the different side chains and how compositionally dependent that tuning effect is as well as the impact on electronic and physical properties. These copolymers are intended to serve as a model system to understand how changes in the primary structure of such polymers through incorporation of functionalized side chains will affect their properties. This work provides a more broad-scope comparison than previous studies in literature looking into how effective different functional groups are in tuning polymer surface energy as a route to allow more strategic synthesis of polymers for binary and ternary blend solar cells.

Results and Discussion

As depicted in Scheme 1, the functional groups investigated in this study are: ester, ether, diether, carbamate and nitrile. These were chosen based on their hydrophilic nature which should increase the surface energy as well as synthetic ease. The synthetic strategy for the family of polymers was guided by our previous findings showing that modifications of polymer side chains that maintained an unfunctionalized two-carbon spacer in between the aromatic core and the functional moiety are effective in tuning surface energy while maintaining electronic and optical properties of the parent polymer.^{30,31}



Scheme 2: General direct arylation polymerization procedure for all co-polymers.

The monomers were copolymerized with 2-Bromo-3-hexylthiophene via DArP as shown in Scheme 2 using $\text{Pd}(\text{OAc})_2$ as the catalyst, K_2CO_3 as the base and neodecanoic acid (NDA) as the acid additive in dimethylacetamide (DMA) at 70 °C to give copolymers with 25% and 50% of the functionalized side chain as well as the P3HT homopolymer. The values of 25% and 50% refer to the molar feed ratio of the comonomers in the polymerization. The exact ratios of functionalised comonomers in the copolymers as determined from $^1\text{H-NMR}$ are listed in Table S3 in the ESI. For the polymers listed as 50% copolymers, the actual functional comonomer content was found to be 46–57%, while for the 25% copolymers, the actual composition was found to range from 21–22%. Detailed conditions for all polymerizations are given in the ESI and are analogous to conditions we have previously reported.^{49–52} Utilization of DArP was crucial in synthesizing copolymers bearing such a large variety of functional groups considering the notably harsher conditions required to synthesize the monomers needed for more traditional polymerization procedures such as *Stille* polymerizations.^{53,54} As such, this study is a good example of the high functional group tolerance of DArP. Moreover, DArP methodologies are highly compatible with the random-polymer-approach employed in these polymerizations for ensuring incorporation of a well-defined amount of the

functionalized comonomer into the respective copolymer.^{55,56} Molecular weights, dispersities (\mathcal{D}), and yields for all polymerizations are listed in Table 1. The copolymers are labelled by their functional group and its content in the copolymers in percent: est = ester, carb = carbamate, eth = ether, nit = nitrile, dieth = diether. All polymers were obtained in decent to high yields with good molecular weights of ≥ 10 kDa which has been shown to be the threshold molecular weight where optical and electronic properties in P3HT largely saturate.^{57,58} Notably, polymers incorporating the nitrile functionalized side chains yielded the lowest molecular weights. Control experiments on nitrile-functionalized polymers with longer reaction times and higher monomer concentrations, listed in Table S3 in the ESI, yielded polymers with higher molecular weights but at the expense of a significantly increased dispersity. We suspect that the known coordination of nitriles to $\text{Pd}(\text{II})$ complexes, specifically $\text{Pd}(\text{OAc})_2$, via their π -bond is interfering with the polymerization and effecting the molecular weight and dispersity while the ratios of incorporated nitrile functionalised monomer are interestingly comparable to those for the other functional groups.^{59–62} Therefore, the nitrile polymers in Table 1 were used for all characterization.

Table 1: Molecular weights, dispersities (\mathcal{D}), yields, surface energies, electrochemical HOMO values, d-spacings and SCLC hole mobilities of P3HT and all ten co-polymers.

Entry	Polymer	M_n [kDa] ^a	\mathcal{D} ^b	Yield ^c	Surface energy [mN/m] ^d	HOMO [eV] ^e	d-spacing [Å] ^f	μ_h mobility [$\text{cm}^2 \text{V}^{-1} \text{s}^{-1}$] ^g
1	P3HT	10.8	2.26	53%	21.3	5.37	16.23	$(2.45 \pm 0.22) \cdot 10^{-3}$
2	P3HT-est-50	14.7	3.49	38%	24.6	5.33	-	$(6.22 \pm 0.39) \cdot 10^{-5}$
3	P3HT-est-25	12.9	2.88	39%	22.8	5.39	16.08	$(5.39 \pm 0.39) \cdot 10^{-4}$
4	P3HT-carb-50	13.3	2.91	76%	28.6	5.27	16.92	$(4.79 \pm 0.53) \cdot 10^{-6}$
5	P3HT-carb-25	14.1	2.89	62%	25.5	5.30	16.92	$(1.69 \pm 0.18) \cdot 10^{-4}$
6	P3HT-eth-50	16.1	2.99	38%	22.3	5.41	16.98	$(5.21 \pm 1.23) \cdot 10^{-4}$
7	P3HT-eth-25	14.0	3.09	40%	21.8	5.24	16.66	$(8.52 \pm 1.47) \cdot 10^{-4}$
8	P3HT-nit-50	9.6	3.38	57%	24.9	5.12	-	$(3.96 \pm 0.54) \cdot 10^{-5}$
9	P3HT-nit-25	7.3	3.51	56%	23.4	5.23	-	$(3.45 \pm 0.24) \cdot 10^{-4}$
10	P3HT-dieth-50	29.0	2.47	56%	25.7	5.36	16.41	$(1.35 \pm 0.51) \cdot 10^{-4}$
11	P3HT-dieth-25	18.7	2.91	34%	22.8	5.34	16.32	$(6.28 \pm 0.96) \cdot 10^{-4}$

^aMolecular weights as determined by SEC calibrated to polystyrene standards after purification by Soxhlet. ^bAs determined by SEC.

^cYield after Soxhlet extraction with methanol, hexanes and reprecipitation from the chloroform fraction. ^dMeasured for neat, as-cast polymer films. ^eDetermined by cyclic voltammetry (vs. Fc/Fc^+) in 0.1M TBAPF_6 in acetonitrile solution. ^fDetermined from GIXRD measurements. ^gMeasured for neat, as-cast polymer films.

Surface energies for the polymers were determined using a contact angle goniometer to measure the contact angles of the respective liquids on pristine, as-cast polymer films. Surface energies were calculated based both on a one-liquid method with water as the probe liquid and a two-liquid approach, using water and glycerol, based on the Wu model.^{46,63} Both sets of data are available in the ESI. For this study we elected to discuss the surface energies based on the one-liquid method for consistency with our previous reports on P3HT-based copolymers. Moreover, large variations in surface energy measurements based on the two-liquid method can be observed when there are dispersion and compatibility issues with one of the solvents and some of the sample polymers.^{31,64,65} To avoid this limitation with the commonly used solvent diiodomethane due to potential solubilizing issues on solid conjugated polymer films, our group switched to glycerol in the past but especially for ether containing polymers glycerol has also been found to pose a solubilizing problem, and thus the one-liquid data is most applicable over the whole family of polymers.³¹

The resulting surface energies for all polymers are shown in Table 1 and a comparative analysis is illustrated in Figure 1. Across all investigated functionalised side chains an increase in surface energy compared to unfunctionalized P3HT was observed. Further, for every given side chain, the 50% copolymer exhibited a more pronounced increase in surface energy than the 25% copolymer. The carbamate side chain was the most effective for enhancing surface energy with 28.6 mN/m for the 50% and 25.5 mN/m for the 25% copolymer compared to 21.2 mN/m for P3HT. The diether, nitrile and ester side chains all resulted in similar surface energies in their 50% copolymers with 25.7 mN/m, 24.9 mN/m and 24.6 mN/m, respectively, which are close to what can be achieved with only 25% carbamate. The ether side chain is the least effective, resulting in a surface energy of 22.3 mN/m for the 50% and only 21.3 mN/m for the 25% copolymer, the latter value which is virtually identical to that of P3HT.

Surface energy is related to a number of properties in polymers including crystallinity, morphology, the surface roughness of the material, and the intrinsic dipole moment of the respective functional group.⁶⁶⁻⁶⁹ When looking at the dipole moments of the functional moieties investigated in this study a rough correlation can be drawn that a higher dipole moment tends to lead to a more pronounced effect on the surface energy. Ethers have the lowest dipole moments, 1.2-1.6 D, followed by esters, 1.8-1.9 D, carbamates, 2.3-2.5 D, and finally nitriles, 3.5-4.0 D.⁷⁰⁻⁸¹ Noticeably, the functional group leading to the highest surface energies, the carbamate, does not have the highest dipole moment demonstrating that other factors such as surface roughness will have to be considered as well for a deeper understanding of the effectiveness of each of the functional groups in tuning surface energy.

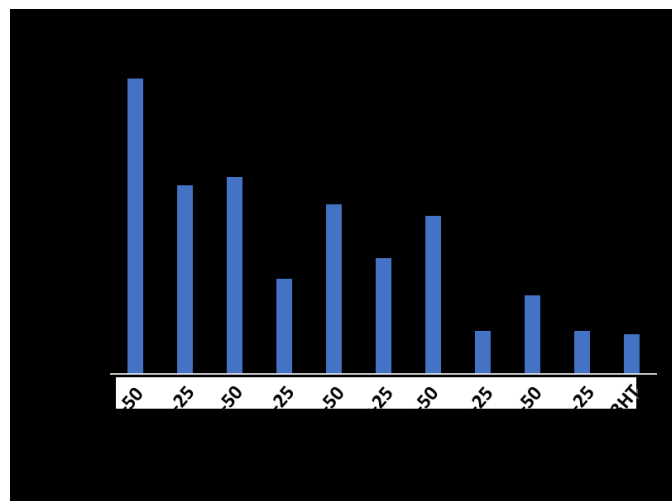


Figure 1: Surface energies of P3HT and all ten copolymers from as-cast thin films.

Beyond changes in surface energy, it is important to understand how the side chains influence basic physical and electronic properties. Ideally, changes in surface energy should be accompanied by minimal changes in other properties. Here we

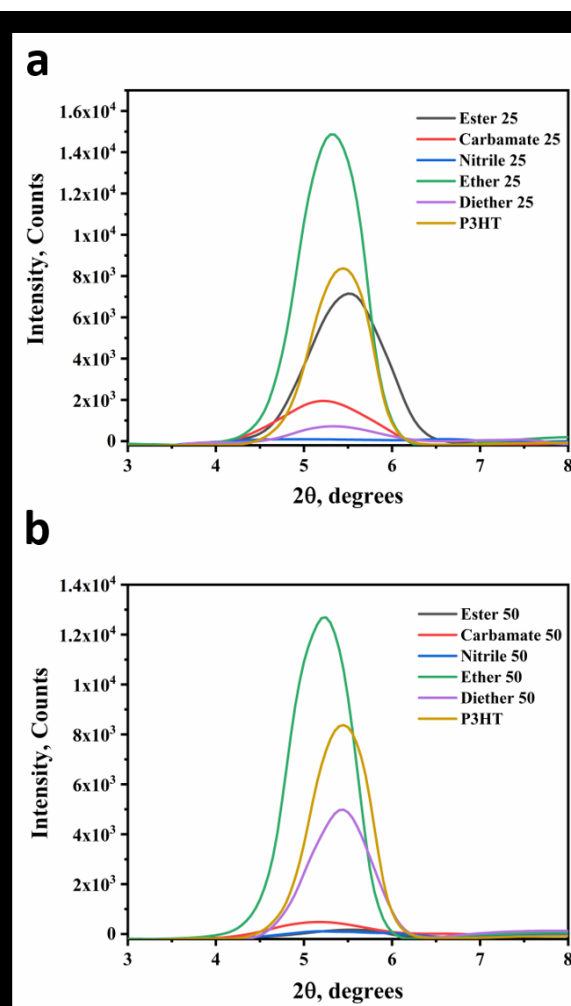


Figure 2: (a) GIXRD data for all 25% copolymers and P3HT, (b) GIXRD data for all 50% copolymers and P3HT. All films were measured as cast.

examine crystallinity via grazing incidence X-ray diffraction (GIXRD) and differential scanning calorimetry (DSC), as well as electronic properties via thin film UV-Vis absorption, HOMO energies via cyclic voltammetry (CV), and hole mobility via the space-charge current limited technique. For GIXRD and UV-Vis absorption measurements unannealed polymer films were used since the optimal annealing conditions can be expected to vary significantly across the family of copolymers due to the nature of the very different side chains, and thus we elected to not to pursue the optimization of annealing conditions.

In Figure 2a the GIXRD data for all 25% copolymers as well as for P3HT is shown. While the peak intensities in GIXRD cannot directly be correlated to %-crystallinity without considering film densities, precedence in conjugated polymer literature indicates that they do serve as an indicator for the levels of crystallinity in the corresponding copolymers.⁸²⁻⁸⁵ Here P3HT-eth-25 shows the most intense peak surpassing even unfunctionalized P3HT. P3HT-est-25, P3HT-dieth-25 and P3HT-carb-25 all show peak intensities that are lower than that of P3HT while P3HT-nit-25 shows virtually no peak. Figure 2b shows the GIXRD data for all 50% copolymers as well as for P3HT. Again, the ether functionalized copolymer shows the most intense peak followed by P3HT and P3HT-dieth-50. All other 50% copolymers show peaks with a distinctly lower intensity.

While neither the P3HT-nit-25 or P3HT-nit-50 samples showed any peaks, the general trend was an observed decrease in peak intensities when going from 25 to 50% of the functionalized side chain for a given functional group. This decrease was dramatic for the ester (Figure S40, ESI) and significant for the carbamate (Figure 43, ESI), but minimal for the ether (Figure S39, ESI). This suggests an increased disruption of the crystalline packing of P3HT as more hexyl side chains are replaced with functionalised side chains with differing steric demands and polarities. In contrast, the diether polymers showed a dramatic increase in peak intensity as diether content increased from 25 to 50%, which is consistent with our previous results.³¹ These results from GIXRD are consistent with the DSC data which showed endothermic peaks upon heating for all 25% copolymers but only for the 50% ether and diether copolymers. The high peak intensity for both ether copolymers suggests appreciable levels of crystallinity. This is consistent with previous findings both by our group and in literature for similar P3HT-derived polymers containing ether functionalized side chains and is most likely due to the interplay of a decreased steric demand of the ether side chains compared to unfunctionalized hexyl side chains.^{30,31,86} Overall both in terms of chain length and steric demand of the side chain the ether and diether containing copolymers are structurally the most similar to P3HT which could serve as an explanation as to why those polymers, especially in the 50% copolymers, show peak intensities that are significantly closer to that of P3HT than all other copolymers. However, the origins of the different trends in GIXRD data for the ether and diether copolymers is not clear nor intuitive.

From the GIXRD data the lamellar (100) d-spacings listed in Table 1 were calculated. While the 50% ester and the nitrile

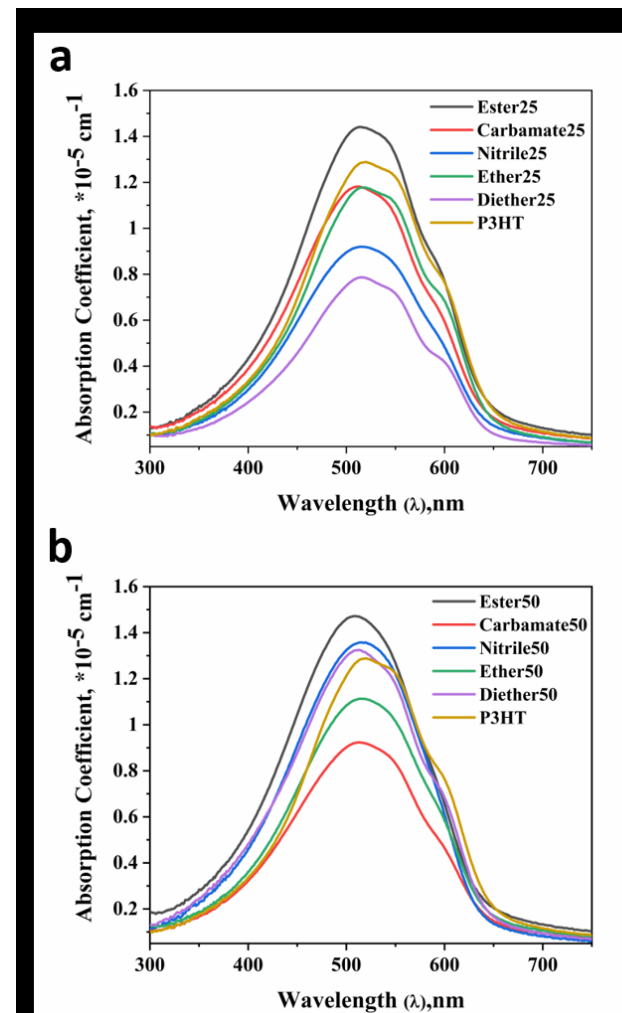


Figure 3: (a) absorption profiles of all 25% copolymers and P3HT and (b) absorption profiles of all 50% copolymers and P3HT. All films were measured as cast.

copolymers did not show a high enough degree of crystallinity to allow for their d-spacings to be calculated, P3HT-eth-50 had the most pronounced effect on d-spacing, increasing it by 0.75 Å when compared to P3HT. Both carbamate copolymers which show virtually identical d-spacing, had almost as pronounced an effect on d-spacing increasing it by 0.7 Å. For P3HT-eth-25, P3HT-dieth-50 and P3HT-dieth-25, d-spacings were only slightly increased, 0.1-0.3 Å, while in P3HT-est-25 d-spacing was decreased by 0.2 Å compared to P3HT. Interestingly, there is no clear correlation between the functional group impact on the polymer alkyl-alkyl packing, as indicated by changes in the d-spacing, and the functional groups impact on the degree of crystallinity. For instance, the ether functionalized side chain shows a very similar, high degree of crystallinity for both the 25% and the 50% copolymer. However, the 50% ether copolymer has a significantly higher impact on d-spacing than the 25% ether copolymer. Further, the copolymers bearing the sterically more demanding carbamate group show a similarly high impact on d-spacing but their crystallinity, especially in P3HT-carb-50, is distinctly lower than in the ether copolymers. The ester functional group, sterically most similar to the carbamate, on the other hand causes a decrease in d-spacings by 0.2 Å instead of an increase by 0.7 Å.

The optical properties of the polymers were investigated by UV/Vis-absorption in thin films. In Figure 3a the absorption profiles for all 25% copolymers and P3HT are shown. The highest absorption was observed for P3HT-est-25, followed by P3HT and then P3HT-carb-25 and P3HT-eth-25 showing very similar absorption profiles. The lowest absorption was measured for P3HT-dieth-25. The low absorption observed for the diether copolymers is in agreement with previous reports showing a decrease in absorption for such copolymers compared to P3HT.³¹

In Figure 3b the absorption profiles for all 50% copolymers and P3HT are shown. Again, the ester copolymer shows the highest absorption followed by the nitrile and the diether with very similar absorption coefficients and then P3HT. The lowest absorption was observed for P3HT-carb-50. In P3HT and P3HT-dieth-50 shoulders in the absorption profiles similar to the 25% analogues in Figure 3a can be seen, but P3HT-eth-50 shows a distinctly reduced vibronic shoulder relative to the corresponding 25% copolymer.

When comparing Figures 3a and 3b, there is no clear trend in the absorption behaviour. With the exception of the ether and carbamate, the 50% copolymers show higher absorption than the 25% analogues, although with the ether and ester the difference between 25 and 50 is minimal. In general, the intensity of the vibronic shoulder was observed to decrease upon increasing functionalized side chain content from 25 to 50%. This is consistent with a decrease in crystallinity at higher side chain contents, which is consistent with the GIXRD and DSC data presented, except for the case of the diether copolymers. A direct comparison of the absorption for the 25% and 50% copolymers for each functional group is presented in Figures S34-S37 in the ESI.

For each polymer, the wavelengths of maximum absorbance (λ_{\max}) and the wavelengths of the onset absorbance (λ_{onset}) were determined from UV-Vis absorptions profiles and the band gaps, E_g , were calculated which are listed in Table S4 in the ESI. All copolymers had a band gap that was in a narrow range of ± 0.02 eV around the band gap of P3HT at 1.89 eV and the λ_{\max} of all polymers fall in the range of 649-662 nm, which is very close to P3HT (656 nm).

To further investigate the electronic properties of the copolymers cyclic voltammetry (CV) was performed and the HOMO energies for all polymers were calculated and shown in Table 1. Relative to P3HT (HOMO = 5.37 eV), most of the polymers show very similar HOMO energies in the range of 5.30-5.40 eV. P3HT-eth-25 shows a higher HOMO of 5.24 eV, which could be explained by the elevated crystallinity of this polymer. However, P3HT-eth-50 is also highly crystalline and shows a HOMO energy of 5.40 eV, close to that of P3HT. The noticeably higher HOMO levels for the nitrile copolymers could be in part due to the substantially lower molecular weights though a deeper correlation is not evident.

Finally, the hole mobilities, μ_h , for all polymers were measured by the space-charge-limited current (SCLC) method. The highest mobility was measured for neat P3HT, $2.45 \cdot 10^{-3}$ cm²V⁻¹s⁻¹, while

all of the 25% copolymers have comparable mobilities that are decreased by about an order of magnitude. The mobilities for the 50% copolymers of the ether, $(5.21 \pm 1.23) \cdot 10^{-4}$ cm²V⁻¹s⁻¹, and diether, $(1.35 \pm 0.51) \cdot 10^{-4}$ cm²V⁻¹s⁻¹, are similar to those observed for the 25% copolymers, while for the ester and nitrile the 50% copolymers show mobilities that are decreased by an order of magnitude compared to their respective 25% copolymers. For the carbamate containing polymers the 50% copolymer has a mobility of $(4.79 \pm 0.53) \cdot 10^{-6}$ cm²V⁻¹s⁻¹ is decreased by two orders of magnitude compared to the 25% copolymer. While there is no clear correlation of mobility with crystallinity, it is clear that increasing amounts of functionalized side chain lead to decreasing mobility as a general trend.

Overall, the incorporation of 25% of functional side chain does not strongly impact the thin film absorption characteristics of the polymers in terms of band gap and vibronic features and leads to only small variations in HOMO energy. Likewise, most of the 25% polymers, with the exception of the low molecular weight P3HT-nit-25, retain crystalline order in the pristine polymer films. In contrast, the 50% copolymers generally show a marked decrease in the vibronic shoulder of the absorption spectra and with the exception of the diether polymers, a decrease in crystallinity is observed relative to their 25% analogues. The general trends observed indicate the higher functional group content is more disruptive and also leads to lower mobilities.

Conclusion

In summary, this work represents a study of the effect of functionalized side chains in P3HT-based random copolymers on surface energies as well as the optical and electronic properties, crystallinity, and hole mobilities. We synthesized a family of ten copolymers featuring five different functional groups on the side chain, an ester, an ether, a carbamate, a nitrile and a diether, which were incorporated in a 25% and in a 50% ratio. Each functional moiety was separated from the conjugated backbone of the polymer by a two-carbon spacer. For all functionalized side chains an increase in surface energy was observed compared to P3HT which was more pronounced in the 50% copolymers than in the 25% copolymers. The carbamate was the most effective in tuning surface energy increasing it from 21.2 mN/m for P3HT to 28.6 mN/m in P3HT-carb-50. Generally, a higher ratio of functionalized side chains seems to lead to lower crystallinity and mobility, but the spacer in between the functional group and the conjugated backbone allowed for the optical, physical and electronic of P3HT to be largely maintained in the 25% copolymers, but to a lesser extent in the 50% copolymers. P3HT-carb-25 stands out as the most promising system due to maintained crystallinity and reasonable mobility while offering the same level of surface energy tuning as what can be achieved with 50% of other functional groups. P3HT-dieth-50 was slightly more effective in tuning surface energy while maintaining a higher degree of crystallinity at a better molecular weight and dispersity than

P3HT-carb-25 but requires a significantly higher ratio of the functionalised sidechain to accomplish that. However, at the same ratio the diether copolymers were noticeably less effective than the carbamate analogues. In the future, this work can serve as a guide for a more strategic and planned approach to tuning polymer surface energies via side chain engineering.

Conflicts of interest

There are no conflicts to declare.

Acknowledgements

We acknowledge funding from the National Science Foundation (CBET-1803063 and MSN-1904650). We also thank Malancha Gupta for use of the contact angle goniometer.

Notes and references

- 1 B. C. Thompson, J. M. J. Fréchet, *Angew. Chem. Int. Ed.*, 2008, **47**, 58.
- 2 R. Søndergaard, M. Hösel, D. Angmo, T.T. Larsen-Olsen, F.C. Krebs, *Mater. Today*, 2012, **15**, 36.
- 3 M. P.Tsang, G. W. Sonnemann, D. M. Bassani, *Prog. Photovoltaics*, 2016, **24**, 645.
- 4 Z. Qiu, B. A. G. Hammer, K. Müller, *Prog. Polym. Sci.*, 2020, **100**, 101179.
- 5 Y. Sui, Y. Deng, T. Du, Y. Shi, Y. Geng, *Mater. Chem. Front.*, 2019, **3**, 1932.
- 6 K. Mahesh, S. Karpagam, K. Pandian, *Topics Curr. Chem.*, 2019, **337**, 12.
- 7 M. Pandey, N. Kumari, S. Nagamatsu, S. S. Pandey, *J. Mater. Chem. C*, 2019, **7**, 13323.
- 8 M. Wang, P. Baek, A. Akbarinejad, D. Barker, J. Travas-Sejdic, *J. Mater. Chem. C*, 2019, **7**, 5534.
- 9 E. M. Speller, A. J. Clarke, J. Luke, H. K. H. Lee, J. R. Durrant, N. Li, T. Wang, H. C. Wong, J.-S. Kim, W. C. Tsoi, Z. Li, *J. Mater. Chem. A*, 2019, **7**, 23361
- 10 C. Lee, S. Lee, G.-U. Kim, W. Lee, B. J. Kim, *Chem. Rev.*, 2019, **119**, 8028.
- 11 Y. Cui, H. Yao, J. Zhang, T. Zhang, Y. Wang, L. Hong, K. Xian, B. Xu, S. Zhang, J. Peng, Z. Fei, F. Gao, J. Hou, *Nat. Commun.*, 2019, **10**, 2515.
- 12 B. Fan, D. Zhang, M. Li, W. Zhong, Z. Zeng, L. Ying, F. Huang, Y. Cao, *Sci. China. Chem.*, 2019, **62**, 746.
- 13 J. Yuan, Y. Zhang, L. Zhou, G. Zhang, H.-L. Yip, T.-K. Lau, X. Lu, C. Zhu, H. Peng, P. A. Johnson, M. Leclerc, Y. Cao, J. Ulanski, Y. Li, Y. Zou, *Joule*, 2019, **3**, 1140.
- 14 R. A. J. Janssen, J. Nelson, *Adv. Mater.* 2013, **25**, 1847.
- 15 N. Gasparini, A. Salleo, I. McCulloch, D. Baran, *Nature Rev. Mater.*, 2019, **4**, 229.
- 16 P. Bi, X. Hao, *Solar RRL*, 2019, **3**, 1800263.
- 17 H. Hwang, D. H. Sin, C. Park, K. Cho, *Sci. Rep.*, 2019, **9**, 12081.
- 18 L. Lu, M. A. Kelly, W. You, L. Yu, *Nat. Photonics*, 2015, **9**, 491.
- 19 B. M. Savoie, S. Dunaisky, T. J. Marks, M. A. Ratner, *Adv. Energy Mater.*, 2015, **5**, 1400891
- 20 P. P. Khlyabich, B. Burkhart, B. C. Thompson, *J. Am. Chem. Soc.* 2011, **133**, 14534.
- 21 P. P. Khlyabich, B. Burkhart, B. C. Thompson, *J. Am. Chem. Soc.* 2012, **134**, 9074.
- 22 R. A. Street, D. Davies, P. P. Khlyabich, B. Burkhart, B. C. Thompson, *J. Am. Chem. Soc.* 2013, **135**, 986.
- 23 K. Yao, Y.-X. Xu, F. Li, X. Wang, L. Zhou, *Adv. Opt. Mater.* 2015, **3**, 321.
- 24 L. Lu, W. Chen, T. Xu, L. Yu, *Nat. Commun.* 2015, **6**, 7327.
- 25 M. Koppe, H.-J. Egelhaaf, G. Dennler, M. C. Scharber, C. J. Brabec, P. Schilinsky, C. N. Hoth, *Adv. Funct. Mater.* 2010, **20**, 338.
- 26 P. P. Khlyabich, A. E. Rudenko, R. A. Street, B. C. Thompson, *ACS Appl. Mater. Interfaces*, 2014, **6**, 9913.
- 27 R. Lin, M. J. Y. Tayebjee, G. Conibeer, M. Wright, *Sol. RRL*, 2017, **1**, 1700035.
- 28 M. Zhang, J. Wang, X. Ma, J. Gao, C. Xu, Z. Hu, L. Niu, F. Zhang, *APL Mater.*, 2020, **8**, 090703.
- 29 N. Gobalasingham, S. Noh, J. B. Howard, B. C. Thompson, *ACS Appl. Mater. Interfaces*, 2016, **8**, 27931.
- 30 J. B. Howard, S. Ekiz, S. Noh, B. C. Thompson, *ACS Macro Lett.*, 2016, **5**, 977.
- 31 J. B. Howard, S. Noh, A. E. Beier, B. C. Thompson, *ACS Macro Lett.*, 2015, **4**, 725.
- 32 K. Jiang, G. Zhang, G. Yang, J. Zhang, Z. Li, T. Ma, H. Hu, W. Ma, H. Ade, H. Yan, *Adv. Energy Mater.*, 2018, **8**, 1701370.
- 33 H. Wu, H. Fan, S. Xu, L. Ye, Y. Guo, Y. Yi, H. Ade, X. Zhu, *Small*, 2019, **15**, 1804271.
- 34 N. Yi, Q. Ai, W. Zhou, L. Huang, L. Zhang, Z. Xing, X. Li, J. Zeng, Y. Chen, *Chem. Mater.*, 2019, **31**, 10211.
- 35 M. Kim, J. Lee, D. H. Sin, H. Lee, H. Y. Woo, K. Cho, *ACS Appl. Mater. Interfaces*, 2018, **10**, 25570.
- 36 J. Gao, W. Gao, X. Ma, Z. Hu, C. Xu, X. Wang, Q. An, C. Yang, X. Zhang, F. Zhang, *Energy Environ. Sci.*, 2020, **13**, 958.
- 37 H. Kang, K.-H. Kim, J. Choi, C. Lee, B. J. Kim, *ACS Macro. Lett.*, 2014, **3**, 1009.
- 38 P. P. Khlyabich, A. E. Rudenko, B. C. Thompson, Y.-L. Loo, *Adv. Funct. Mater.*, 2015, **25**, 5557.
- 39 R. A. Street, P. P. Khlyabich, A. E. Rudenko, B. C. Thompson, *J. Phys. Chem. C*, 2014, **118**, 26569.
- 40 X. Du, T. Heumueller, W. Gruber, O. Almora, A. Classen, J. Qu, F. He, T. Unruh, N. Li, C. J. Brabec, *Adv. Mater.*, 2020, **32**, 1908305.
- 41 P. Maisch, L. M. Eisenhofer, K. C. Tam, A. Distler, M. M. Voigt, C. J. Brabec, H.-J. Egelhaaf, *J. Mater. Chem. A*, 2019, **7**, 13215.
- 42 J. Wang, Z. Zheng, D. Zhang, J. Zhang, J. Zhou, J. Liu, S. Xie, Y. Zhao, Y. Zhang, Z. Wei, J. Hou, Z. Tang, H. Zhou, *Adv. Mater.*, 2019, **31**, 1806921.
- 43 S. Lee, K. H. Park, J.-H. Lee, H. Back, M. J. Sung, J. Lee, J. Kim, H. Kim, Y.-H. Kim, S.-K. Kwon, K. Lee, *Adv. Energy Mater.*, **9**, 1900044.
- 44 L. Huang, G. Wang, W. Zhou, B. Fu, X. Cheng, L. Zhang, Z. Yuan, S. Xiong, L. Zhang, Y. Xie, A. Zhang, Y. Zhang, W. Ma, W. Li, Y. Zhou, E. Reichmanis, Y. Chen, *ACS Nano*, 2018, **12**, 4440.
- 45 H. Zhang, Y. Li, X. Zhang, Y. Zhang, H. Zhou, *Mater. Chem. Front.*, 2020, **4**, 2863.
- 46 Y. Sun, S.-C. Chien, H.-L. Yip, K.-S. Chen, Y. Zhang, J. A. Davies, F.-C. Chen, B. Lin, A. K.-Y. Jen, *J. Mater. Chem.*, 2012, **22**, 5587.
- 47 Q. Wang, Z. Hu, Z. Wu, Y. Lin, L. Zhang, L. Lin, Y. Ma, Y. Cao, J. Chen, *Appl. Mater. Interfaces*, 2020, **12**, 4659.
- 48 S. Cong, A. Creamer, Z. Fei, S. A. J. Hillman, C. Rapley, J. Nelson, M. Heeney, *Macromol. Biosci.* 2020, **20**, 2000087.
- 49 A. E. Rudenko, C. A. Wiley, S. M. Stone, J. F. Tannaci, B. C. Thompson, *J. Polym. Sci. A Polym. Chem.*, 2012, **50**, 3691.
- 50 A. E. Rudenko, B. C. Thompson, *Macromolecules*, 2015, **48**, 569.
- 51 A. E. Rudenko, A. A. Latif, B. C. Thompson, *J. Polym. Sci. A Polym. Chem.*, 2015, **53**, 1492.

52 A. E. Rudenko, B. C. Thompson, *J. Polym. Sci. A Polym. Chem.*, 2015, **53**, 2494.

53 N. S. Gobalasingham, B. C. Thompson, *Prog. Polym. Sci.*, 2018, **83**, 135.

54 A. E. Rudenko, B. C. Thompson, *J. Polym. Sci. A Polym. Chem.*, 2015, **53**, 135.

55 A. E. Rudenko, P. P. Khlyabich, B. C. Thompson, *ACS Macro Lett.*, 2014, **3**, 387.

56 N. S. Gobalasingham, R. M. Pankow, S. Ekiz, B. C. Thompson, *J. Mater. Chem. A*, 2017, **5**, 14101.

57 A. Zen, J. Pflaum, S. Hirschmann, W. Zhuang, F. Jaiser, U. Asawapirom, J. p. Rabe, U. Scherf, D. Neher, *Adv. Funct. Mater.* 2004, **14**, 757-764.

58 A. M. Ballantyne, L. Chen, J. Dane, T. Hammant, F. M. Braun, M. Heeney, W. Duffy, I. McCulloch, D. D. C. Bradley, J. Nelson, *Adv. Funct. Mater.* 2008, **18**, 2373-2380.

59 Y. Ping, L. Wang, Q. Ding, Y. Peng, *Adv. Synth. Cat.* 2017, **359**, 3274-3291.

60 B. Corain, S. Rancan, M. Zecca, S. Lora, G. Palma, *J. Mol. Catal.* 1989, **55**, 209-219.

61 N. V. Kaminskaia, N. M. Kostić, *J. Chem. Soc., Dalton Trans.* 1996, **18**, 3677-3686.

62 K. Yamamoto, H. Sogawa, T. Takata, *Polym. J.* 2021, **53**, 565-571.

63 X. Bulliard, S.-G. Ihn, S. Yun, Y. Kim, D. Choi, J.-Y. Choi, M. Kim, M. Sim, J.-H. Park, W. Choi, K. Cho, *Adv. Funct. Mater.*, 2010, **20**, 4381.

64 R. N. Shimizu, N. R. Demarquette, *J. Appl. Polym. Sci.*, 2000, **76**, 1831.

65 M. Zenkiewicz, *JAMME*, 2007, **24**, 137.

66 D. K. Owens, R. C. Wendt, *J. Appl. Polym. Sci.*, 1969, **13**, 1741.

67 F. Zhang, E. Mohammadi, X. Luo, J. Strzalka, J. Mei, Y. Diao, *Langmuir*, 2018, **34**, 1109-44.

68 D. E. Packham, *Int. J. Adhes. Adhes.*, 2003, **23**, 437.

69 L. Vitos, A. V. Ruban, H. L. Skriver, J. Kollár, *Surf. Sci.*, 1998, **411**, 186.

70 B. Bakri, J. Demaison, I. Kleiner, L. Margulès, H. Møllendal, D. Petitprez, G. Włodarczak, *J. Mol. Spectrosc.*, 2002, **213**, 312.

71 R. M. Pontes, E. A. Basso, *J. Mol. Struct.*, 2002, **594**, 199.

72 C. Cox, T. Lectka, *J. Org. Chem.*, 1998, **63**, 2426.

73 C. M. Lee, W. D. Kumler, *J. Am. Chem. Soc.*, 1961, **83**, 4596.

74 M. Heraïl, M. Berthelot, A. Proutiere, *J. Phys. Org. Chem.*, 1995, **8**, 421.

75 S. K. Dev, S. R. Landor, C. W. N. Cumper, *J. Chem. Soc., Perkin Trans.*, 1973, **2**, 537.

76 T. Gramstad, K. Tjessem, *J. Mol. Struct.*, 1977, **41**, 231.

77 B. Krishna, S. K. Bhargava, B. Prakash, *J. Mol. Struct.*, 1971, **8**, 195.

78 E. Salz, J. P. Hummel, P. J. Flory, M. Plavšić, *J. Phys. Chem.*, 1981, **85**, 3211.

79 T. Uchida, Y. Kurita, M. Kubo, *J. Polym. Sci.*, 1956, **19**, 365.

80 R. A. Spurr, H. Zeitlin, *J. Am. Chem. Soc.*, 1950, **72**, 4832.

81 A. Kotera, K. Suzuki, K. Matsumura, T. Nakano, T. Oyama, U. Kambayashi, *Bull. Chem. Soc. Jpn.*, 1962, **35**, 797.

82 T. Kim, J. Choi, H. J. Kim, W. Lee, B. J. Kim, *Macromolecules* 2017, **50**, 6861-6871.

83 J. Oh, K. Kranthiraja, C. Lee, K. Gunasekar, S. Kim, B. Ma, B. J. Kim, S.-H. Jin, *Adv. Mater.* 2016, **28**, 10016-10023.

84 H. You, D. Kim, H.-H. Cho, C. Lee, S. Chong, N. Y. Ahn, M. Seo, J. Kim, F. S. Kim, B. J. Kim, *Adv. Funct. Mater.* 2018, **28**, 1803613.

85 C. Lee, T. Giridhar, J. Choi, S. Kim, Y. Kim, T. Kim, W. Lee, H.-H. Cho, C: Wang, H. Ade, B. J. Kim, *Chem. Mater.* 2017, **29**, 9407-9415.

86 L. Chen, W. Liu, Y. Yan, X. Su, S. Xiao, X. Lu, C. Uher, X. Tang, *J. Mater. Chem. C*, 2019, **7**, 2333.